Mechanical Properties of Solid-State Resistance Welded Nitinol - 304 Stainless Steel Joints in Peripheral Guide Wires

A Senior Project Presented to

The Faculty of the Materials Engineering Department

California Polytechnic State University, San Luis Obispo

In Partial Fulfillment of the Requirements for the Degree

Materials Engineering, Bachelor of Science

by

Jennifer Rowe

June 2016

Table of Contents

ABSTRACT

Abbott Vascular manufactures medical guide wires that consist of 304 stainless steel wire joined to superelastic nickel titanium (Nitinol) wire by a solid-state resistance butt welding process. The objective of this project was to develop a deeper understanding of the mechanical properties of the welds in the guide wires. The wires tested were manufactured using two different processes and then ground to various diameters in the weld region. Vickers microhardness measurements were collected in the longitudinal direction across the heat-affected zones of the welds, as well as the transverse direction across the diameters of the welds. Micrographs of the welds produced by each of the two processes were generated in order to develop a fuller understanding of the where the indentations were relative to the flow of the welds. Wires with 304 stainless steel - Nitinol (NiTi) joints were tensile tested to determine if process type and grind diameter have affect ultimate tensile strength. Wires welded using Process A and ground to 0.0125″ had a mean ultimate tensile strength of 192.11ksi, whereas these wires ground to 0.0055″ had a mean ultimate tensile strength of 174.68ksi. Wires welded using Process B and ground to 0.0125″ had a mean ultimate tensile strength of 179.79ksi, whereas Process B wires ground to 0.0055″ had a mean ultimate tensile strength 158.47ksi. Analysis shows that process type and grind diameter independently affect the mechanical properties of the welded joints in the guide wires.

Key Words: Nitinol, Shape Memory, Superelasticity, 304 Stainless Steel, Fusion Welding, Solid-State Resistance Welding, Materials Engineering, Tensile Testing Wires, Microhardness

1. ACKNOWLEDGEMENTS

Thank you to Professor Blair London, in the Materials Engineering Department for his guidance and support as my advisor for this project. Thank you to John Simpson from Abbott Vascular for sponsoring the project, including manufacturing the samples and acting as a valuable resource regarding anything guide wire-related. Thank you to Professor Jeffrey Sklar from the Statistics Department, who consulted with me regarding the statistical analysis of the results.

2. LIST OF FIGURES

3. LIST OF TABLES

4. INTRODUCTION

Medical guide wires are extremely fine wires (on the order of 0.010″in diameter) that surgeons insert and direct through the human cardiovascular system in order to guide and place medical devices, such as balloon catheters and stents (Figure 1). The development of medical guide wire technology has greatly expanded the number and types of procedures that can be executed with a percutaneous approach. Using a percutaneous approach can reducing recovery time, allowing patients to return to their normal schedules and responsibilities more quickly than invasive surgical procedures. [1]

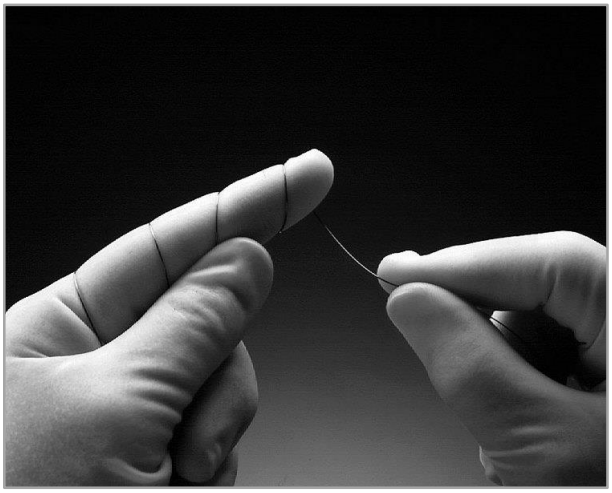

Figure 1. An example of a Nitrex guide wire, a peripheral guide wire with a Nitinol core. The elasticity of the wire is showcased by wrapping it around a finger. [2]

The reduction in recovery time makes critical preventative procedures more accessible to patients who cannot afford to take long periods of time away from their daily responsibilities. In a 2013 study of 23,814 employed patients, one portion of the patients underwent minimally invasive procedures and the remaining patients underwent standard, open surgical approach procedures. The patients who had the minimally invasive procedures missed 9 to 37.7 fewer days (mean values with a 95% confidence interval) of work depending on their particular procedure. As well as missing less days of work, the mean health plan spending for the minimally invasive procedures was $1,350 to $30,850 lower than the comparable open surgical approach procedures. [1]

The placement of peripheral stents using medical guide wires, is one such common percutaneous procedure that is minimally invasive. Unique peripheral guide wires that are relatively new to the medical industry have been developed to manage the difficulties of placing devices in patients' extremities. [3] [4] These guide wires consist of a proximal section of 304 stainless steel wire joined to a distal section of Nitinol. Producing wires that have a stainless steel section of wire welded to a Nitinol section of wire (two core materials) enable physicians to utilize the stiffness of stainless steel when steering the guide wire, and the superelasticity of the Nitinol end to avoid kinking while navigating the tortuous paths of the vascular system (Figure 2). Welding Nitinol to stainless steel is difficult, as the two materials have significantly different properties. Attempted fusion welding processes have commonly resulted in weak welds. Abbott Vascular (Temecula, CA) has successfully used a solid-state resistance butt welding process to join the two metals for use in guide wires through a proprietary process.

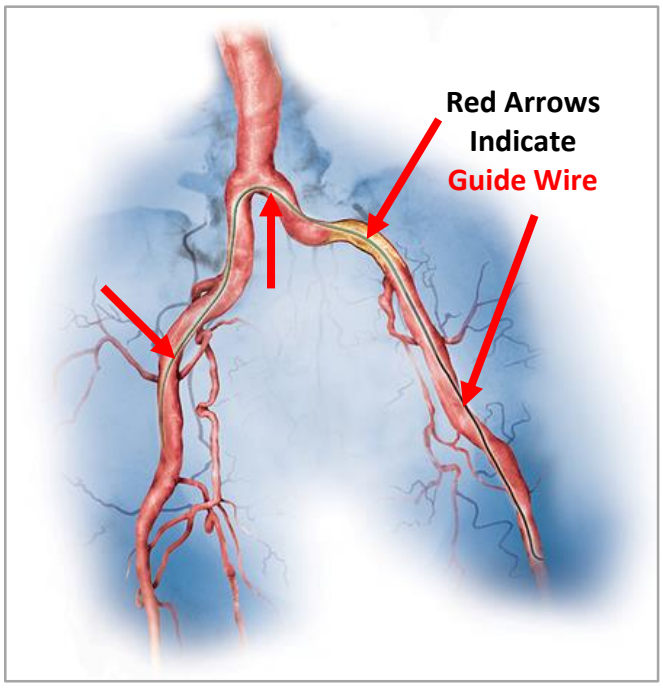

Figure 2. Illustration showing a Terumo Glidewire Advantage peripheral guide wire navigated through small vessels. [5]

4.1 Nitinol in Guide Wires

Nitinol is a nickel-titanium alloy containing about 50 atomic percent nickel and 50 atomic percent titanium. The thermal shape memory and superelastic properties of Nitinol make the material ideal for various unique engineering applications, including use in medical guide wires. A martensitic phase transformation in Nitinol enables the material to recover from relatively large amounts of deformation. This transformation can be induced either thermally or mechanically, and serves as the mechanism for these unique properties. [6]

4.1.1 Thermal Shape Memory (Shape Memory Effect)

Nitinol exhibits a shape memory effect when it undergoes a thermally activated martensitic phase transformation. In this transformation, austenite transforms to martensite as the material cools from an elevated temperature. The martensite is softer and more pliable that the austenitic phase. The martensite returns to austenite, and the original device geometry, once reheated to a sufficiently high temperature (Figure 3). [6] Nitinol medical guide wires do not implement thermal shape memory capabilities. This phase transformation is, however, taken advantage of in devices such as Nitinol stents.

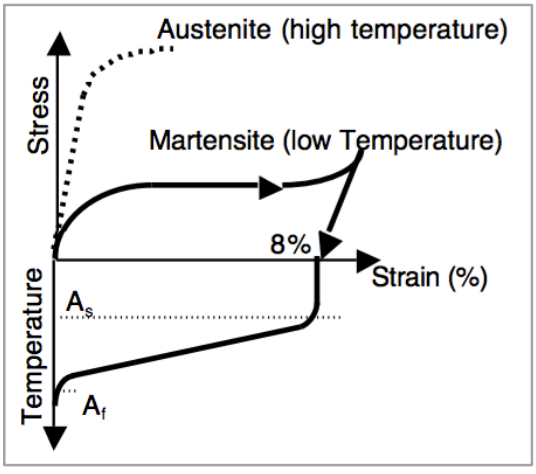

Figure 3. Stress-strain diagram showing the thermally activated martensitic transformation that associated with the shape memory properties in Nitinol. [6]

4.1.2 Superelasticity

The martensitic phase transformation associated with Nitinol's superelasticity can also be induced by the application of stress to the material. In this phase transformation, austenitic Nitinol transforms into stress-induced martensite. When the applied stress is removed, the stress-induced martensite transforms back into austenite (Figure 4). This mechanical event is referred to as non-linear superelasticity and does not require thermal activation. The mechanism of superelasticity in medical guide wires is stress-induced phase transformation. [6]

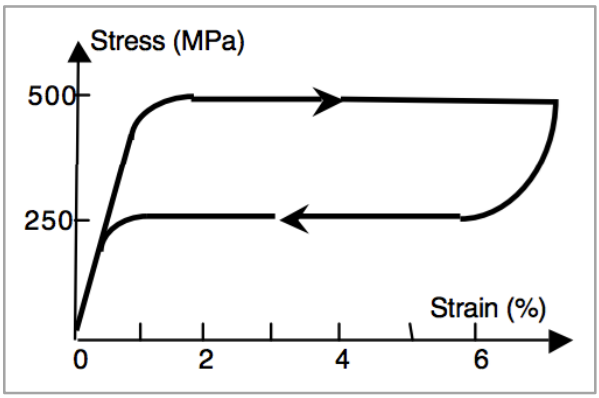

Figure 4. Stress-strain diagram showing the superelastic effects of the stress-induced martensitic phase transformation. [6]

4.2 304 Stainless Steel Overview

One of the most common alloys of stainless steel is 304 stainless steel. This steel is an austenitic steel containing about 18-20 weight percent chromium and 8-10.5 weight percent nickel, with a remaining balance of iron. [7] The nickel serves to stabilize the austenitic crystal structure (Face-Centered Cubic, FCC) at room temperature. The chromium enables the formation of a protective oxide layer. This steel is commonly used for its corrosion resistance and formability. [8]

4.2.1 Crystal Structure

The 304 stainless steel used in medical guide wires is heavily cold-worked. The the high degree of cold-work elongates the FCC crystal structure of austenite, transforming portions of the austenitic structure to a tetragonal martensitic structure. Martensite has higher strength and hardness than austenite, and is less formable. The amount of cold-work can be controlled,

enabling better control of wire properties. [8]

4.2.2 Corrosion Resistance

When the surface of stainless steel is exposed to air, the chromium in the alloy quickly reacts with oxygen, forming a thin passive oxide layer. This chromium oxide layer protects against corrosion by acting as physical and electrical barrier to the environment. If the oxide layer is damaged (e.g., scratched, chipped, etc.) a new oxide layer will form at the exposed surface almost instantly, as long as oxygen and sufficient amounts of chromium are present. The rapid nature of the oxide growth is why stainless steel is often referred to as having a "self-healing" oxide.

When used in medical guide wires, the passive layer protects against the harsh environment of the human body. If there are discontinuities in the oxide layer and the stainless steel is placed in a corrosive media, the steel is prone to pitting corrosion (Figure 5). The pits are initiated at the discontinuities in the oxide layer. [8]

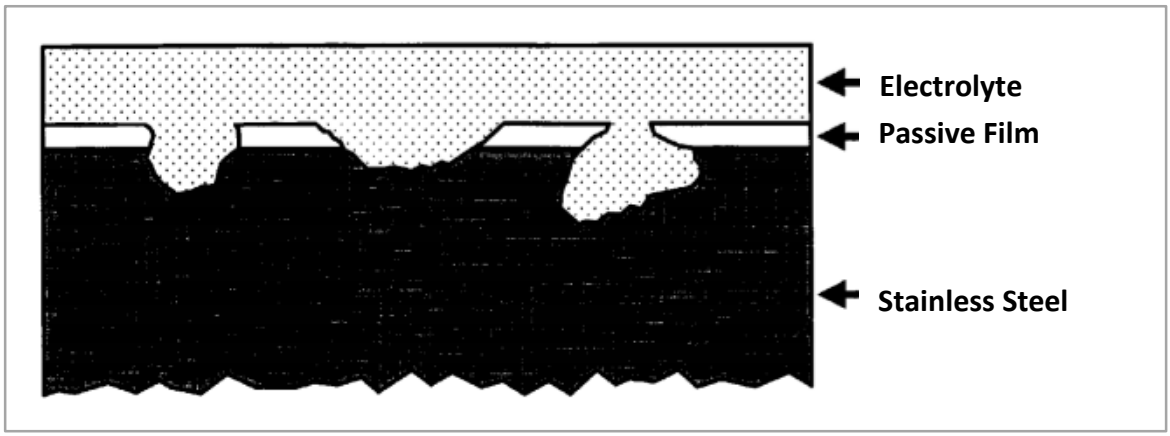

Figure 5. Pitting corrosion in stainless steel due to discontinuities in the passive oxide film. [8]

4.3 Welding Nitinol to 304 Stainless Steel

Both fusion welding and solid-state welding processes have been attempted for joining Nitinol to stainless steel in guide wires. [9] Abbott Vascular has been successful in using a solid-state resistance butt welding process to join the wires.

4.3.1 Fusion Welding

Fusion welding is a general term for joining processes where one or both metals to be joined are heated above their melting temperatures to fuse together. Various fusion welding processes have been attempted when joining stainless steel to Nitinol, including laser welding and electric resistance welding. [10] [11] Three main difficulties arise when attempting to fusion weld stainless steel to Nitinol. Their melting temperatures are significantly different, at 1400°C – 1450°C for 304 stainless steel, and 1240°C – 1310°C for Nitinol. [7] [8] This poses practical challenges when designing weld parameters. The second issue is that brittle intermetallics tend to form in the weld region when the alloys are heated to their melting temperatures, causing the weld to be weak. These fusion welds usually have a clearly defined region in the weld where the two alloys mix. The severe contrast in mechanical properties where the mixed material meets Nitinol wire acts as a nucleation point for fractures (Figure 6). [10] Due to the tortuous pathways of the vascular system, weak fusion welds are not appropriate for guide wire applications.

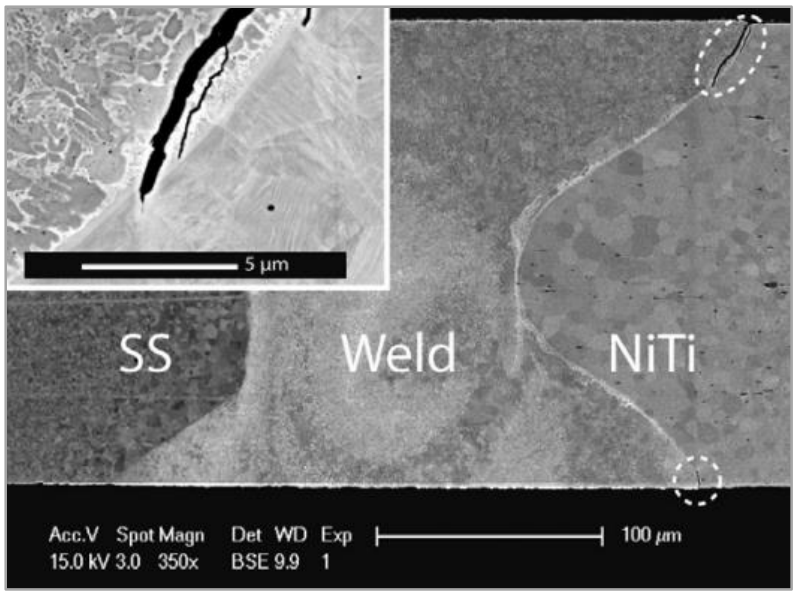

Figure 6. Micrograph taken using Scanning Electron Microscopy with Back Scatter Electron detection. The micrograph shows a longitudinal section of laser welded stainless steel to Nitinol. A crack is highlighted in a dotted white circle and magnified in the upper left hand corner of the figure. [10]

4.3.2 Solid-State Resistance Welding of Wires

In solid-state resistance butt welding, neither of the two alloys are heated to their melting points as they would be in a traditional fusion welding process. Instead, the edges of the two wires that are to be joined, are ground flat and then carefully pressed together, aligning the wires into a flat butt joint configuration. A voltage source is attached to the two wires and current is used to heat them while remaining well below their melting temperatures. As the wires are heated, compressive force is applied to the wires. The combination of heat and pressure causes the wires to bond, forming a solid-state weld. This welding process requires a similar set up to flash butt welding (Figure 7). [11]

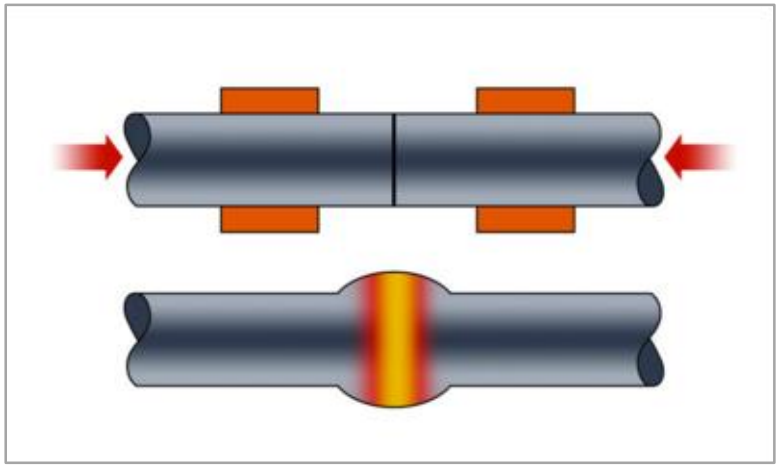

Figure 7. Example set up for flash butt welding process. The top image shows the two wires under compressive force (represented by the red arrows) with a voltage source attached (represented by the orange rectangles). The bottom image shows a heated and bonded weld joint. [11]

For peripheral guide wires that consist of 304 stainless steel and Nitinol sections, the end of a 304 stainless steel wire is welded to the end of a Nitinol wire. The oxide layers on each of the two materials (chromium oxide layer on stainless steel, and titanium oxide layer on Nitinol) prevent the current through the wire from being evenly distributed throughout the cross sections of the two wires. This can cause uneven heat or a lack of sufficient heat at the joint of the weld, causing weld failure. Thus, it is important to remove the oxides just prior to welding. This joining process results in a weld that does not have a region of mixed material between the stainless steel and Nitinol portions (Figure 8).

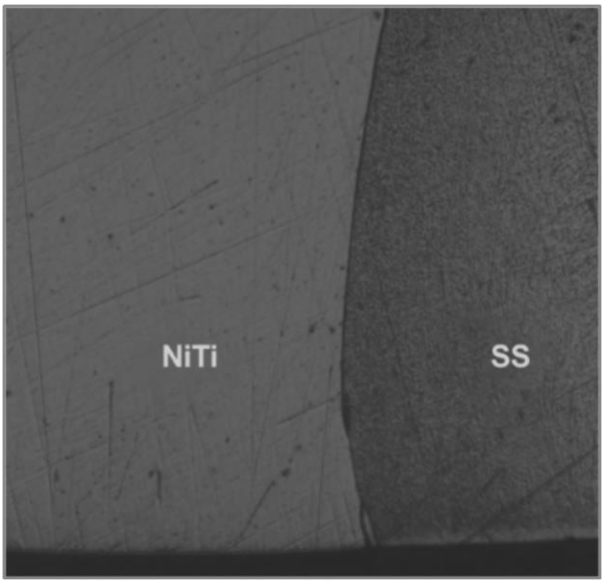

Figure 8. SEM image of a solid-state welded Nitinol (NiTi) and stainless steel (SS) guide wire. The weld has a seamless nature and small grains in the heat-affected zone in the stainless steel section are visible. The stainless steel portion of wire is 0.018″ in diameter and the Nitinol 0.020″ in diameter. The magnification was not provided. [14]

The solid-state welded wires are not raised to the melting temperature of either of the two alloys, preventing the formation of brittle intermetallics in the joint. Also, the Nitinol interfaces directly with the stainless steel, rather than with a region of mixed material, improving the mechanical properties of the weld. Solid-state welding produces welds with improved mechanical properties compared to fusion welding processes, including improvements in strength and ductility. These improvements cause guide wires joined using a solid-state welding process to be better suited for navigating the complex pathways of peripheral cardiovascular systems. [14]

4.4 Biocompatibility

Biocompatibility qualification and testing is essential for any biomedical device. Guide wires are single use devices that are generally in the body for less than two hours. Since peripheral guide wires containing a stainless steel section welded to a Nitinol section are relatively new to industry, there is little literature available reviewing the biocompatibility of the devices in their entirety. Thus, it is important to review the biocompatibility of the device's components to gain insight into the overall device biocompatibility.

4.4.1 Nitinol Biocompatibility

Extensive research is available regarding in vitro and in vivo testing of the biocompatibility of Nitinol. Nitinol contains about 50 atomic percent nickel and 50 atomic percent titanium. Nickel is a known irritant and common allergen. Thus it is essential to determine the amounts of nickel released from Nitinol into the body. Cytotoxicity and corrosion rates of Nitinol have been studied extensively in vitro. Despite higher initial nickel dissolution, the overall metallic ion release was found to have about the same toxicity as stainless steel (low toxicity). In vivo in tests on rats resulted in non-toxic and non-irritant responses from Nitinol in soft tissue. Thus, it would be expected that the Nitinol section of the medical guide wire is biocompatible. [7]

4.4.2 Stainless Steel Biocompatibility

The primary constituents of 304 stainless steel are iron, chromium, and nickel. Similarly to Nitinol (as with any nickel-containing alloy), it is critical to determine the amounts of nickel released from stainless steel medical devices into the body. Testing shows that the toxicity of 304 stainless steel cannot be predicted based on the toxicity of its individual bulk constituents. Instead, the metallic release of stainless steel in various bodily environments must be considered. Since medical guide wires are used in the vascular system, the reaction of stainless steel in blood in vitro is a good indicator of its biocompatibility. There is also extensive research available regarding the reaction of stainless steels in vitro, in urine and sweat tests. [15]

Scientists found that the surface finish of stainless steels greatly affected the release of metallic constituents into the body. Polished surfaces generally release low amounts of nickel into synthetic blood. The exposed stainless steel portion of guide wires are generally polished, and thus can be expected to release low amounts of nickel into the body. The release of other constituents into the body such as chromium and iron are also low, within safe levels. These metallic release levels are different than the metallic release behavior of the individual bulk constituents. For example, pure nickel and pure iron release more metallic ions into the body than when they are combined with chromium in stainless steel. This is due to the chromium oxide layer limiting the metallic release from the stainless steel. The repeated dose and long term toxicity of stainless steel has also been extensively researched. Since guide wires are not in the

body for repeated or long periods of time (usually a single use of less than two hours), those tests are not necessarily indicative to how guide wires will interact with the body. Overall, stainless steel was found to exhibit low amounts of metallic ion release in various in vitro tests showing it to have low toxicity. [15]

Peripheral guide wires consisting of a length of stainless steel welded to a length of Nitinol are relatively new to the guide wire industry. The combination of the stiff, corrosion resistant stainless steel section with the superelastic guide wire section produce a wire with unique properties that expands the capabilities of guide wires. In order to develop a broad understanding of this new technology, it is important to review the current literature available related to how the device works and the biocompatibility of the device. Extensive information is available regarding the biocompatibility of stainless steel and Nitinol, individually. There are areas of literature that are lacking regarding the biocompatibility of medical guide wires. It is difficult to find any research on the biocompatibility of the type of stainless steel to Nitinol weld used in the dual core guide wires. Furthermore, there is a lack of published literature reviewing the biocompatibility of guide wires (the finished product) that contain a stainless steel - Nitinol joint.

4.5 Problem Statement

Abbott Vascular (Temecula, CA) would like to develop a deeper understanding of the mechanical properties of the solid-state resistance butt welds in their peripheral guide wires. They would like to compare the mechanical properties of wires produced by two different manufacturing processes, at various weld diameters. Prior work in this area has shown that guide wires tend to fail at the welds during tensile tests, indicating that the material is weakest at the welds. Developing a further understanding the effects of process type and weld diameter on the mechanical properties will assist with future guide wire design considerations. The following mechanical tests were conducted: tensile tests of the wires, microhardness measurements in the longitudinal direction across the heat-affected zones of the welds, and microhardness measurements in the transverse direction across the diameters of the welds. Statistical analysis on the ultimate tensile strength was used to provide insight into whether or not the data is statistically significant, and aids in comparing the data of the two different manufacturing processes. Micrographs of the welds produced by each of the two processes were generated to

develop a fuller understanding of the microstructures and flow lines relative to the microhardness values.

5. EXPERIMENTAL PROCEDURE

5.1 Tensile Testing

The tensile testing output variable was maximum tensile load on the wire before failure. There were two factors and multiple levels of each factor for the tensile sample groups. The two factors were process type, and grind diameter. There were two levels of weld processes: Process A and Process B.* For tensile testing, there were three levels of grind diameters for the wires welded using Process A: 0.0125" (original grind diameter), 0.0085" and 0.0055". There were four levels of grind diameters for the wires welded using Process B: 0.0145" (original grind diameter), 0.0125", 0.0085" and 0.0055" (Figure 9). Each group had ten samples, for a total of 70 tensile tests. The testing order was randomized using a random number generator in a spreadsheet. Abbott Vascular manufactured the guide wire tensile samples and measured the diameter of each wire using a dual axis laser micrometer.

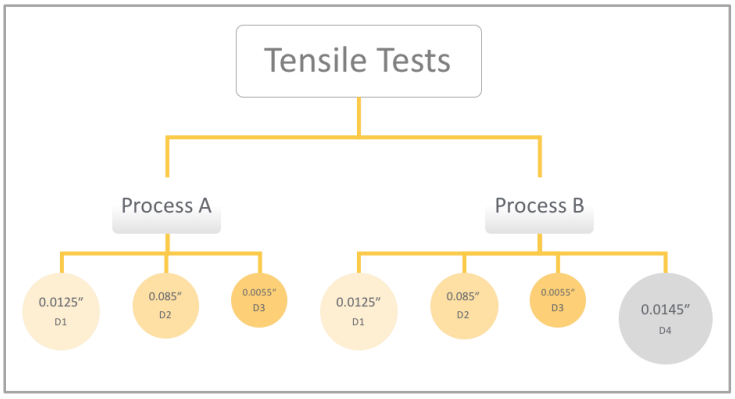

Figure 9. Diagram outlining the tensile testing groups.

In preliminary tests, the wires continually slipped out of the capstan grips before failure. After the manufacturing process is complete, portions of the wires have a Teflon coating. The Teflon

*Details of the processes are proprietary to Abbott Vascular.

reduced the friction between grips and wires. It was manually ground off each tensile sample using 240-grit abrasive paper for subsequent tests. Another issue was that the stainless steel and Nitinol portions of the wires resisted deformation from the grips, possibly due to the strength of the 304 stainless steel portion of wire, the superelasticity of the Nitinol portion of wire, and the relatively low roughness of the grip faces. The 304 stainless steel portion of wire was clamped between 240-grit abrasive paper and the Nitinol clamped between two washers to increase the friction and prevent wire slippage in subsequent tests. Figure 10 shows a wire loaded in the set-up used for all the tensile tests. In this set up the 304 stainless steel was wrapped around the capstan grip approximately 1.5 times, and then clamped in between abrasive paper with the flat faces of the grips. The Nitinol was not wrapped around a grip. Instead, the large D-shaped portion of one of the grips was removed in order to clamp the Nitinol between two washers. This test set-up caused the wires to be loaded at a small angle rather than in strictly uniaxial tension.

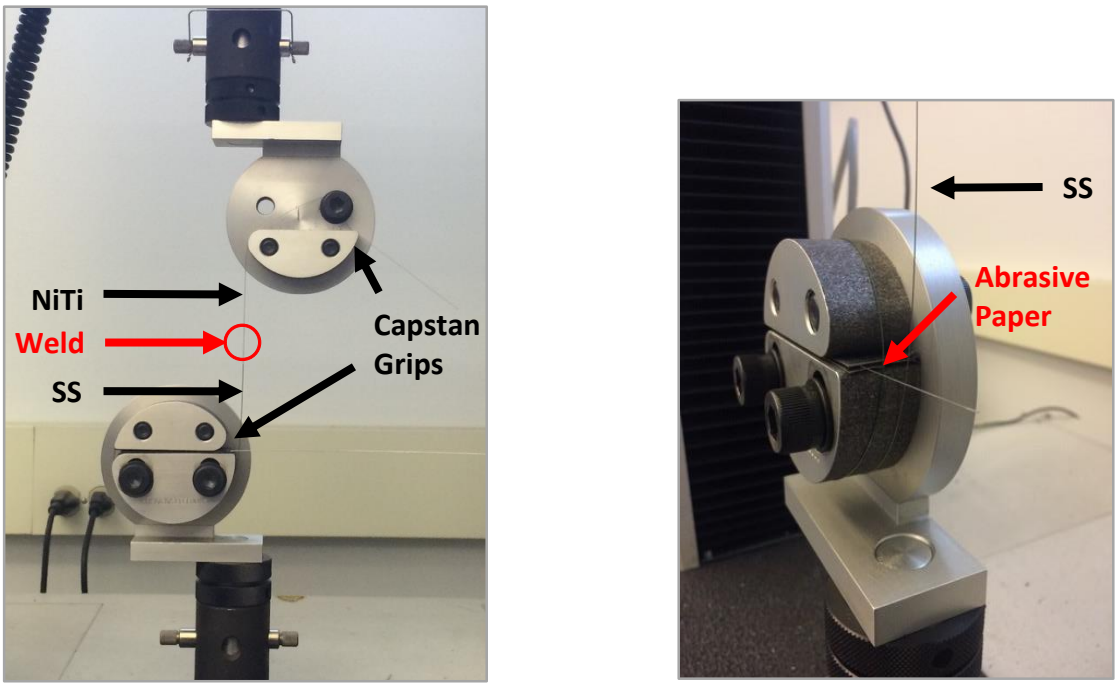

(a) (b)

Figure 10. Tensile test set-up. (a) Sample clamped in two capstan grips, Nitinol portion on top, stainless steel portion on bottom. The red circle indicated the approximate region of the weld. (b) Stainless steel section of wire wrapped around bottom capstan grip and clamped between abrasive paper.

The samples were tested on an Instron tensile tester with a 5kN load cell. The tests were load-controlled, with a load rate of 0.2 lbf per second. The data acquisition rate was set to collect one

data point (load measurement) every 0.1 seconds. The welds were located in the gage length between two grips, which was approximately 5.75". The samples were loaded at a constant rate until fracture. The maximum loads and measured diameters were used to calculate the ultimate tensile strength (UTS) in ksi, of each wire.

5.2 Vickers Microhardness

Due to the small scale of the wires (on the order of 0.010″in diameter) Vickers microhardness indentations were used to measure the hardness values. In order to survey the microhardness across the diameter, the wires had to be mounted, then ground and polished to approximately the mid-plane of the wire (Figure 11). A small section of wire, containing the weld, was cut and mounted using two-part quick set acrylic. The mounted samples had no visible voids in the areas where the acrylic interfaced with the wires.

It was difficult to place the wires parallel to the face of the mounts. Twisting the end of the stainless steel section of wire helped balance the wire flat up against the mold face when pouring the acrylic, and helped prevent the wire from separating from the mount during the abrading and polishing process. The mounted sample was secured in a precision specimen holder. The holder enabled the grind depth of the sample to be set to approximately the mid plane of the sample. Once the depth of grind was set, the sample was abraded using 320-grit, 600-grit, 800-grit, then 1200-grit, in that order until the silicon carbide ring on the specimen holder prevented further material removable which resulted in a planar surface near the mid-plane of the wire. The specimen holder was removed before polishing. The samples were polished using 6-micron abrasive, 1-micron abrasive, and 0.05-micron abrasive colloidal suspensions.

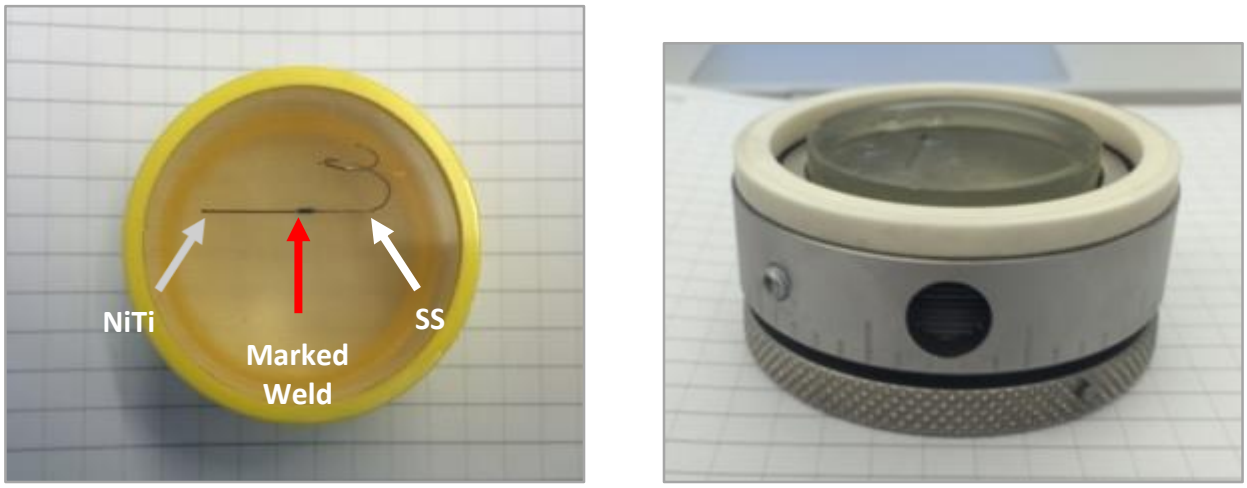

(a) (b)

Figure 11. (a) Wire sample cold mounted in acrylic, showing the orientation of the Nitinol section, stainless steel section, and weld of the wire in the mount. (b) Mounted sample inserted in precision specimen holder prior to grinding and polishing.

Microhardness measurements were collected in the longitudinal and transverse direction for one wire produced using Process A, and one wire produced using Process B. The diagram below shows the general pattern followed for the longitudinal and transverse hardness measurements in both the stainless steel and Nitinol sections of the wires (Figure 12).

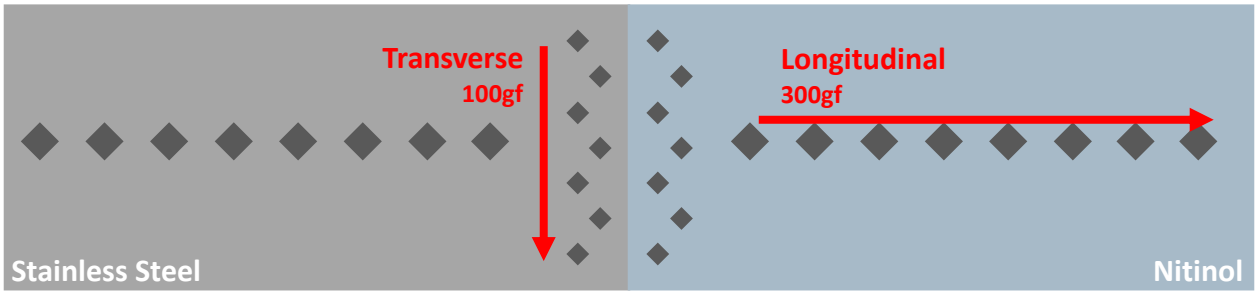

Figure 12. Diagram showing the transverse and longitudinal directions of the wire.

The samples were later etched to expose the flow lines of the welds. The etchant was prepared using high density polyethylene (HDPE) lab equipment, rather that glass lab ware because hydrofluoric acid (HF) dissolves glass. The solution was 5mL HF, 13mL nitric acid (HNO_3), and 75mL distilled water. The surface of each of the two the polished samples were etched for approximately 1-2 minutes. A cotton swab containing the etchant solution was rubbed over the surface until the mirror finish of the Nitinol dulled and darkened in color.

6. RESULTS

6.1 Ultimate Tensile Strength

The values for ultimate tensile strength were calculated using the maximum load from the tensile tests and the measured grind diameters of the wires provided by Abbott Vascular. Table 1 shows the mean ultimate tensile strength (UTS) values for each group. Wires welded using Process A and ground to 0.0125″ had a mean UTS of 192.11 ksi, whereas Process A wires ground to 0.0055″ had a mean UTS of 174.68 ksi. Wires welded using Process B and ground to 0.0125″ had a mean UTS of 179.79 ksi, whereas Process B wires ground to 0.0055″ had a mean UTS 158.47 ksi.

Table I. Mean Ultimate Tensile Strength

Group	Process Types	Target Diameter (inch)	Mean UTS (ksi)
Group 1	A	0.0125	192.11
Group 2	A	0.0085	182.00
Group 3	A	0.0055	174.68
Group 4	B	0.0125	182.96
Group 5	B	0.0085	179.79
Group 6	B	0.0055	171.39
Group 7	B	0.0145	159.59

The UTS values for each tensile test are plotted in Figure 13. The Process A data is blue, and the Process B data is orange. Process A produced wires had higher ultimate tensile strengths than wires with the same diameters produced using Process B. Wires with a grind diameter of 0.0125" have the highest ultimate tensile strengths. Wires with a grind diameter of 0.0085" have a lower ultimate tensile strength than the 0.0125" wires, but a higher ultimate tensile strength than the wires with a grind diameter of 0.0055". The wires with a grind diameter of 0.0055" have the lowest ultimate tensile strength.

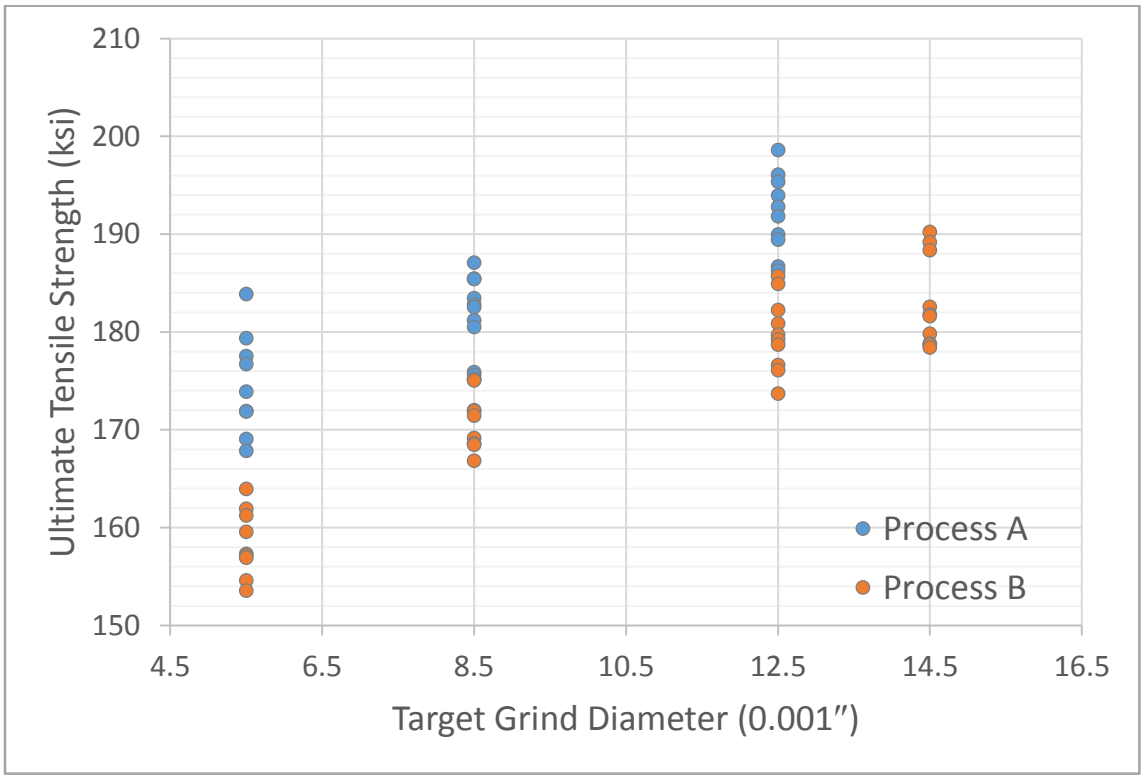

Figure 13. Ultimate Tensile Strength values based on maximum load values collected in tensile tests.

6.2 Microhardness Measurements

Vickers hardness was calculated using the averaged measured diagonals and indenter load of each microindentation measurement. The hardness values measured along the longitudinal direction of the wire, starting in the heat-affected zone near the weld and then moving away from the weld in the Nitinol section of the wire, are shown in Figure 14.

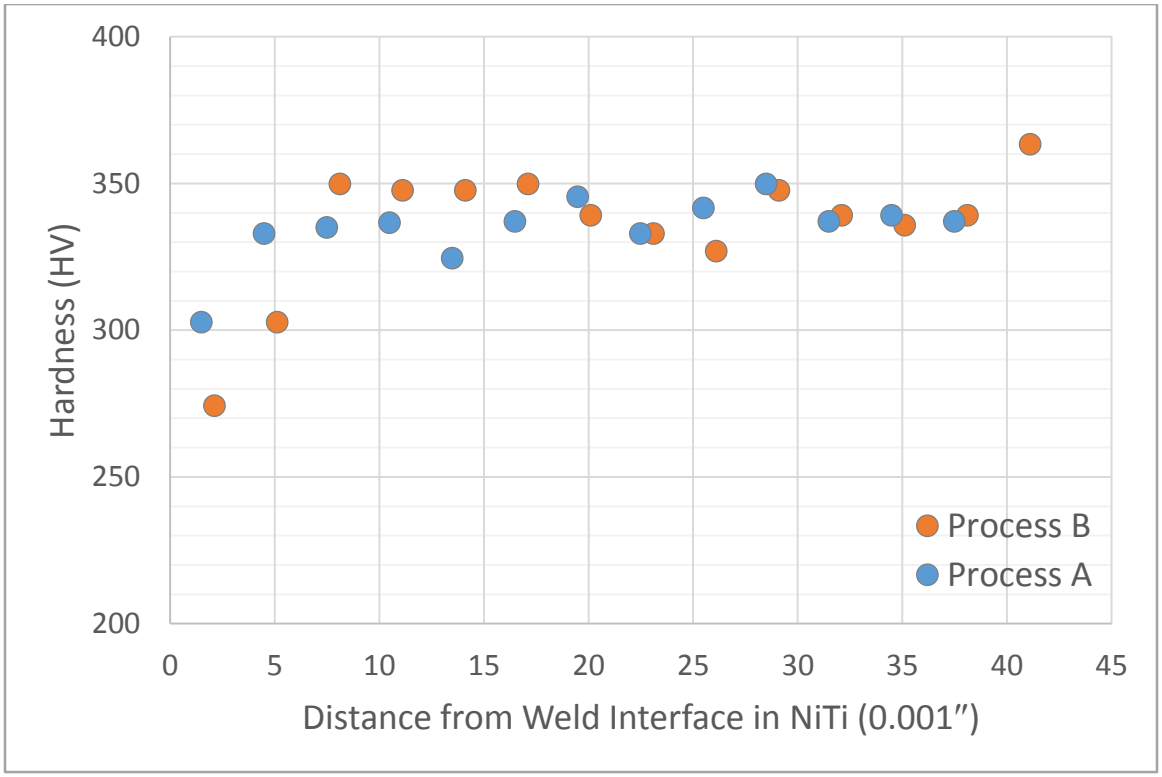

Figure 14. Vickers microhardness values collected in the longitudinal direction of the wires in the Nitinol section.

The hardness values measured across the diameter of the wires near the weld in the Nitinol section of the wire, are shown in Figure 15.

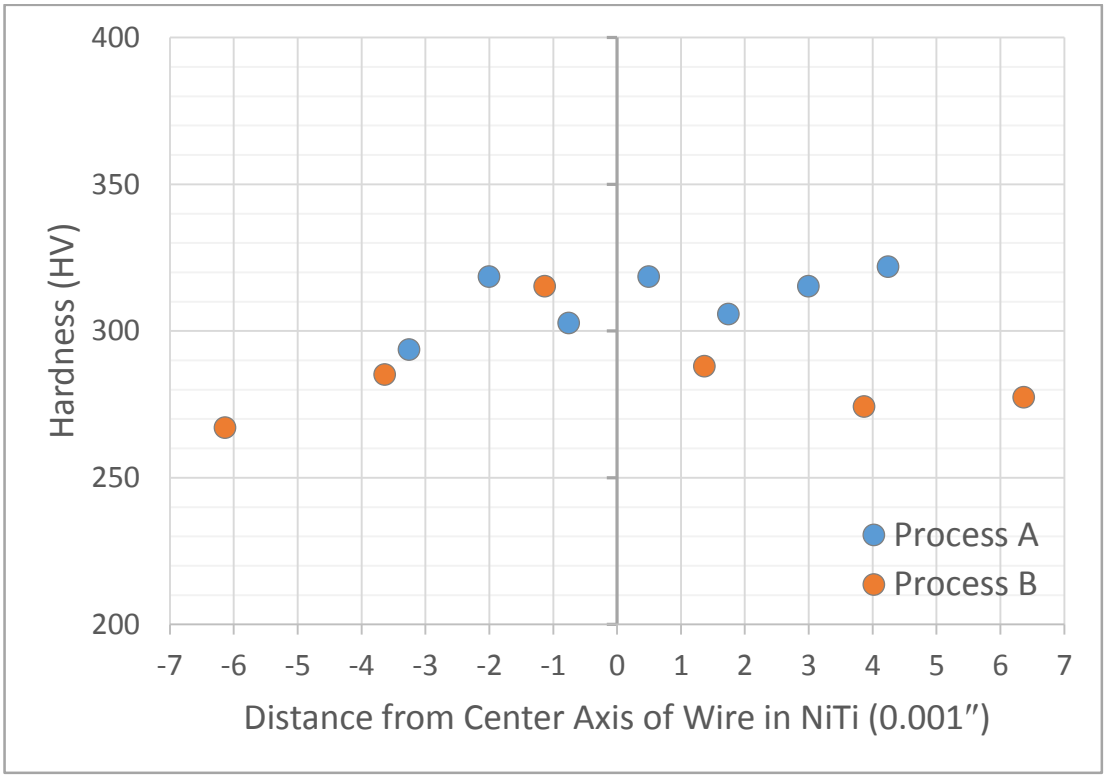

Figure 15. Vickers microhardness values collected in the transverse direction, across the diameter, of the wires in the Nitinol section.

7. ANALYSIS

7.1 Statistical Analysis of Tensile Data

7.1.1 Analysis of Variance

A two-way analysis of variance (ANOVA) was conducted using a general linear model to determine whether process type or weld diameter have significant effects on the ultimate tensile strength of the guide wire welds. The distribution of the residuals was normal and the variance in the data is nearly the same, two assumptions that must be met to proceed with an ANOVA (Figure 16). For this analysis, target grind diameter and process type were considered categorical

factors. Ultimate tensile strength was the response variable. The tensile data for the 0.0145" grind diameter for the Process B wires, was not included in any of the statistical analysis since wires of this diameter were only tested for one of the two process types. Both the process type and diameters had sufficiently low p-values of 0.000 to suggest that each factor independently had a significant affect on ultimate tensile strength. There were no interactions between the two factors.

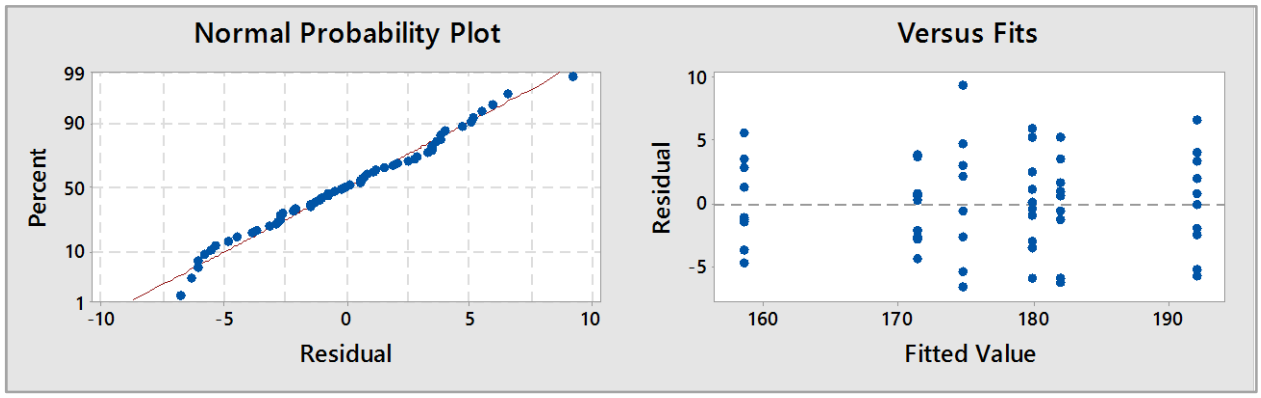

Figure 16. The test for normality residual plot a test for equal variance plot developed prior to ANOVA to determine if data meets the assumptions necessary to use this analysis technique.

7.1.2 Analysis of Covariance

Analysis of Covariance (ANCOVA) is similar to ANOVA, in that it is used to determine whether grind diameter and process type have an affect on ultimate tensile strength. However, in this method, the individually measured grind diameters were used instead of the target grind diameters for each group. Process type was considered a categorical factor, and measured grind diameter was considered a continuous covariate. The response variable was ultimate tensile strength. The data also passed the normality test and test for equal variance, fulfilling the assumptions for this analysis.

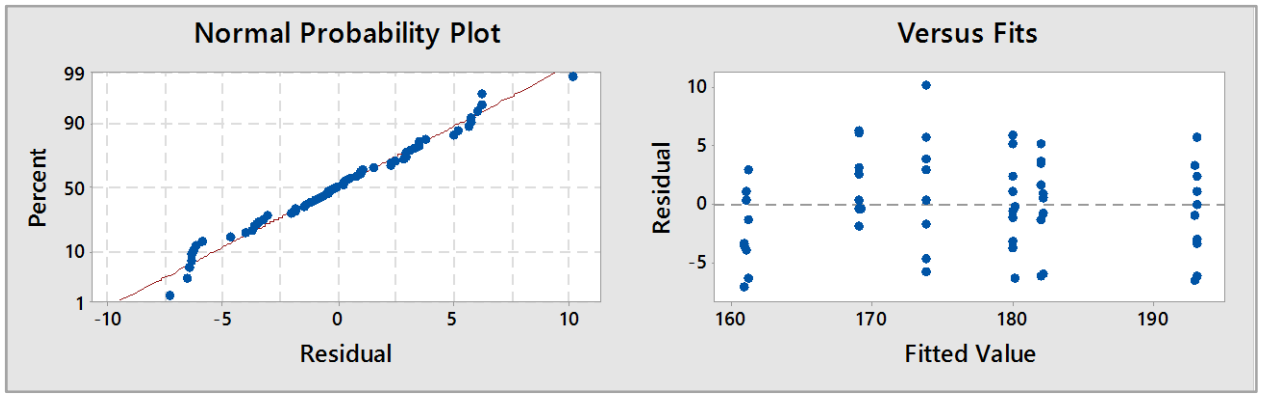

Figure 17. The test for normality residual plot a test for equal variance plot developed prior to ANCOVA to determine if data meets the assumptions necessary to use this analysis technique.

The ANCOVA method resulted in the same conclusions as the ANOVA regarding the effects on process type and grind diameter on ultimate tensile strength. This statistical method can be utilized to produce equations that relate ultimate tensile strength, measured grind diameter, and process type, since measured grind diameter and ultimate tensile strength are both continuous data sets (rather than categorical) (Eq 1 and Eq 2).

$$Process\ A: UTS = 158.39 + 2.778\emptyset \qquad \text{Eq 1}$$

$$Process\ B: UTS = 145.90 + 2.778\emptyset \qquad \text{Eq 2}$$

Where, *UTS* is ultimate tensile strength in ksi, and ϕ is measured grind diameter in inches. These equations are useful in predicting the approximate tensile strengths of guide wires with grind diameters between those tested in this project.

7.1.3 Tukey Comparisons

The Tukey comparison method, is used to develop confidence intervals for all pairwise differences between levels, allowing the levels to be compared within a specified error rate. After the ANOVA and ANCOVA analyses, the first Tukey comparison compared the two process levels (Process A and Process B) to determine if there was a significant difference between the means of the two levels, with a confidence interval of 95%. Table 2 shows results of this comparison, where *N* is the number of samples tested for each level. Since the mean UTS for the

two levels do not share a grouping (denoted by A and B), they are significantly different. That is, the mean UTS of Process A is significantly different than the mean UTS of Process B.

Table II. Tukey Comparison of Process Types

Process Type	N	Mean UTS	Grouping
Process A	29	182.93	A
Process B	29	169.884	B

Figure 18 shows the difference in means for this comparison. There is only one bar of data there are only two levels being compared. The blue point in the middle of the plotted bar represents the mean of the differences, and the length of the bar represents the range in the differences between the levels. Since the bar does not cross zero on the x-axis, the two levels are significantly different.

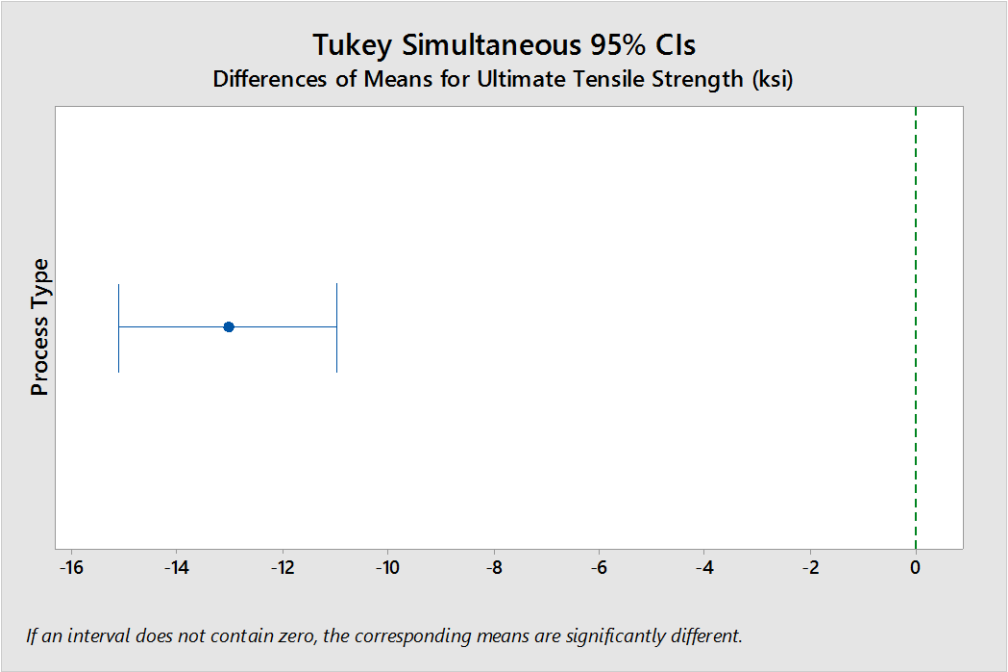

Figure 18. Plot showing the that Process A and Process B have significantly different mean UTS. The difference between the process was calculated by subtracting Process A values from Process B values, causing the negative sign.

The second Tukey comparison was utilized to compared target grind diameter (0.0125", 0.0085", and 0.0055") with a 95% confidence interval. Again, the fourth grind diameter for the Process B wires, 0.0145", was not included in this analysis since wires of this diameter could not be tested

for both levels of process type. Table 3 shows the results of this comparison. None of the mean UTS values for the three levels of diameters shared a grouping (denoted by A, B and C), indicating that they were significantly different.

Table III. Tukey Comparison of Grind Diameters

Target Grind Diameter (0.001")	N	Mean	Grouping
12.5	20	185.949	A
8.5	20	176.697	B
5.5	18	166.577	C

Figure 19 shows the confidence intervals developed by this comparison. There are three bars of data because there are three possible combinations of grind diameters. Since none of the three the bars cross zero on the x-axis, the three levels are all are significantly different.

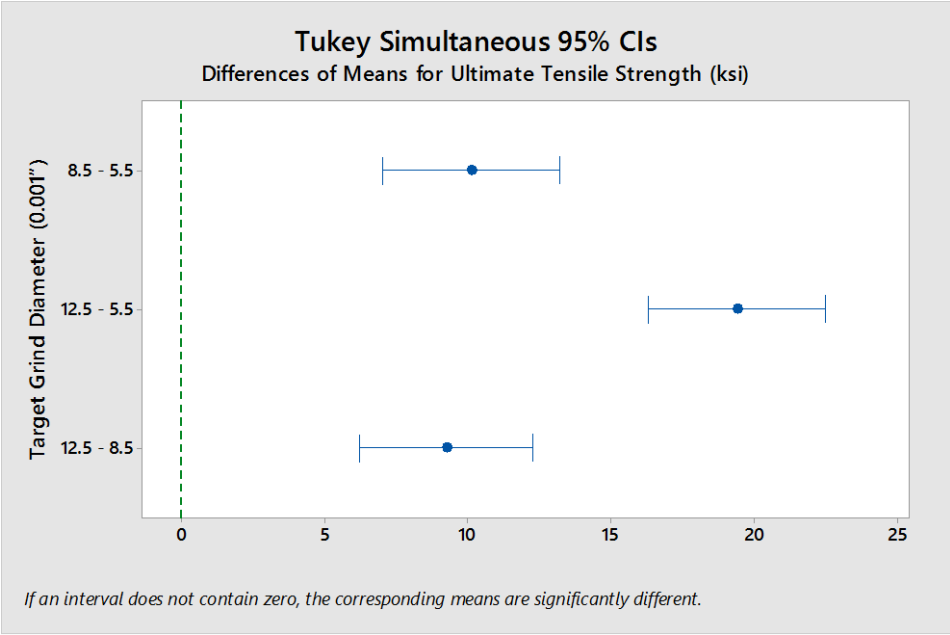

Figure 19. Plot showing that wires with 0.0125", 0.0085", and 0.0055" grind diameters have significantly different mean UTS values. The difference between each grind diameter was calculated, as shown on the y-axis.

The final Tukey comparison compared the all combinations of process type and grind diameter, for a total of 6 groups to determine if there was a significant difference between the means of any of these groups, with a confidence interval of 95%. Table 4 shows results of this comparison. The groups that share a grouping (denoted by A, B, C, D and E) are not significantly different.

Based on this, the mean ultimate tensile strengths of the groups that share the B grouping, are not significantly different. This is also the case for the groups sharing the C and D groupings. All other pairwise comparisons are significantly different.

Table IV. Tukey Comparison of all Tensile Groups

Target Grind Diameter (0.001”)* Process Type	N	Mean UTS	Grouping			
12.5 Process A	10	192.107	A			
8.5 Process A	10	182.005		B		
12.5 Process B	10	179.79		B	C	
5.5 Process A	9	174.68			C	D
8.5 Process B	10	171.389				D
5.5 Process B	9	158.474				E

Figure 20 shows the differences in mean UTS developed by this comparison. There are 15 bars of data because that is the number of possible combinations (without repeats) of the 6 sample groups being compared. Three out of the 15 bars, cross zero on the x-axis, indicating that the mean UTS values are not significantly different. These are the same three groups that shared groupings in Table 4.

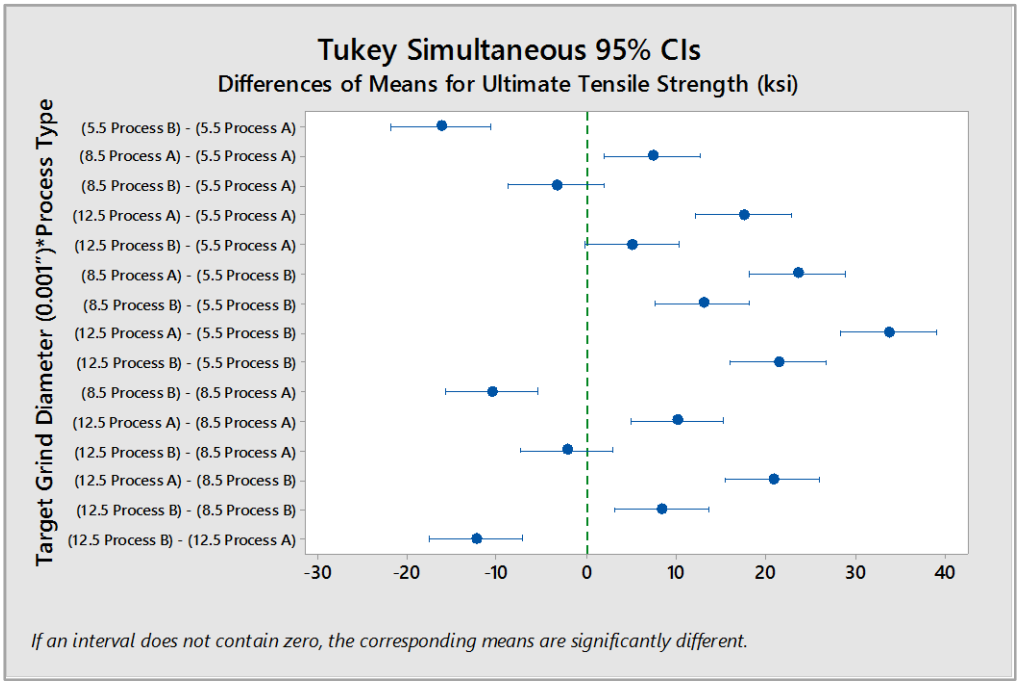

Figure 20. Plot showing the difference in mean values for all combinations of the two process levels (Process A, Process B) with the three grind diameter levels (0.0125", 0.0085", 0.0055"). The bars that cross the zero on the x-axis represent sample groups that do not have significantly difference UTS values.

7.2 Weld Ductility

The 304 stainless steel portion of one of the fractured wires was examined using scanning electron microscopy (SEM) in order to calculate the percent reduction of area of the wire. The wire that was imaged, was tensile sample 62. This was a Process B wire with a target grind diameter of 0.0125" and a measured, original grind diameter of 0.01226". The percent reduction of area was calculated by measuring the original and final diameter of the wire and then directly relating those values to the percent change in cross sectional area (Figure 21). The longer red dashed line shows where the original diameter was measure after fracture, and the short dashed line shows the diameter in the region where fracture occurred. The percent reduction of area was approximately 56.6%.

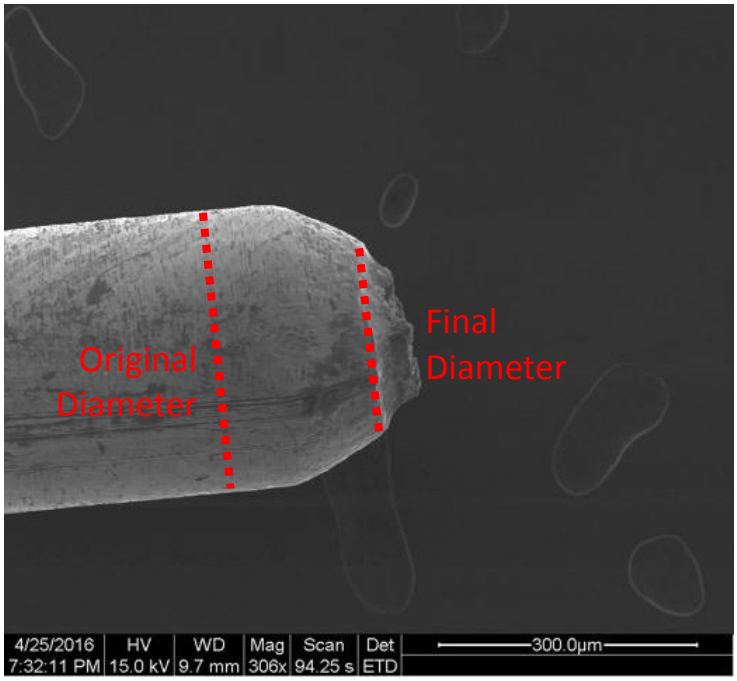

Figure 21. Image showing percent reduction of area measurements of the fracture surface of the stainless steel side of a Process B wire (tensile sample 62). The image was taken using Scanning Electron Microscopy and is at a magnification of 306X.

The fracture surface was imaged at higher magnifications (Figure 22). At these magnifications, significant necking is observed. Also, the topography of the fracture surface is consistent with ductile rupture. The tensile samples fracture near to the weld interface, sometimes slightly in the Nitinol section of wire. The combination of a high percent reduction of area, a clearly necked region, and evidence of ductile rupture indicated that this weld was ductile and underwent plastic deformation.

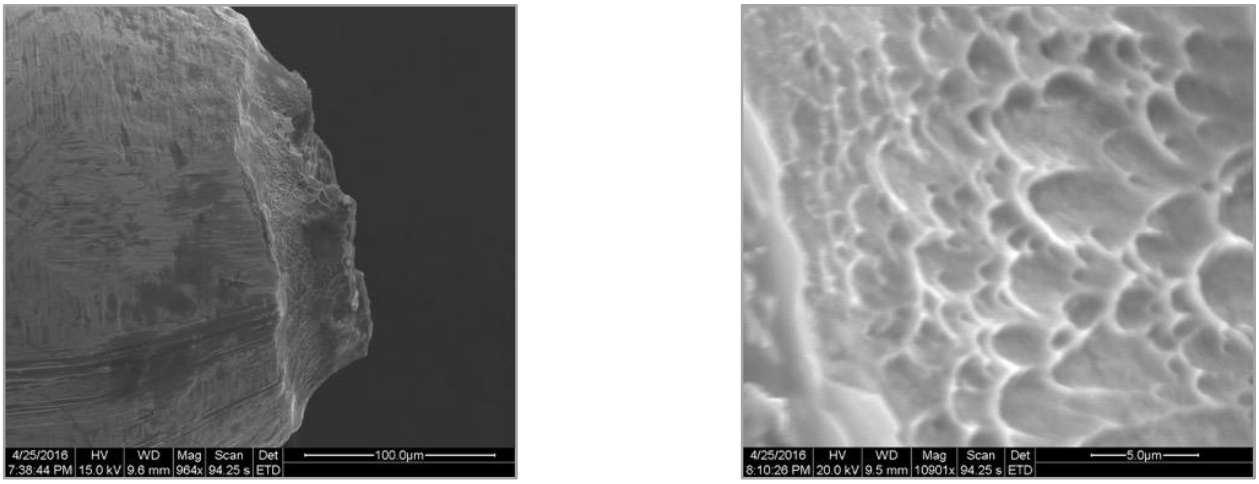

(a) (b)

Figure 22. (a) Fracture surface of wire Sample #62 at a magnification of 964X, using an SEM. (a) Fracture surface of wire Sample #62 at a magnification of 10,901X, using an SEM.

7.3 Bright-field Microscopy of Microhardness Indentations

After microhardness indentations were measured and hardness values calculated on one sample from each process type, the samples were etched to reveal the flow lines of the weld region in the Nitinol portion of the wires. Imaging the microhardness samples with the flow lines visible helped indicate where the heat-affected zone (HAZ) was relative to the microhardness indentations. The micrographs in Figure 23 are of the Process A guide wire. The darker region of the Nitinol seen in Figure 23(a), near the weld interface, corresponds to heat-affected zone in Nitinol. In Figure 23(b) the flow lines were more visible due to the higher magnification. The hardness values were lower in the heat-affected zone and increased until they eventually plateaued, when moving further away from the weld interface. The hardness values across the diameter (in the transverse direction) did not show a trend in hardness.

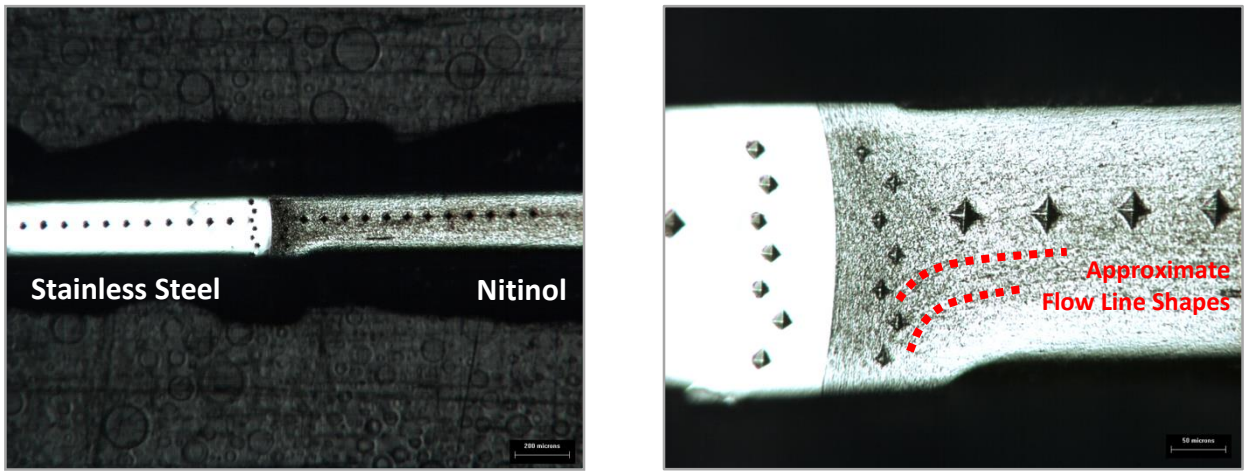

(a) (b)

Figure 23. Process A guide wire (a) 50x magnification (b) 200x magnification. In both micrographs, the Nitinol section is the darker portion of the wire, on the right side of each image.

The micrographs in Figure 24 are of the Process B wire. As with the Process A wire, the darker region of the Nitinol seen in Figure 24(a), near the weld interface, corresponds to heat-affected zone in Nitinol. In Figure 24(b) the flow lines were also more visible. The wire showed a similar trend where the hardness values were lower in the heat-affected zone and increased until they eventually plateaued, when moving further away from the weld interface. One significant difference, is that the hardness remained lower for a longer distance from the weld than the Process A wire. This could indicate that the length of the HAZ in the Process A wire was different (shorter) than the length of the HAZ in the Process B wires. As with the Process A wire, the hardness values across the diameter (in the transverse direction) did not show a trend in hardness in the Process B wire.

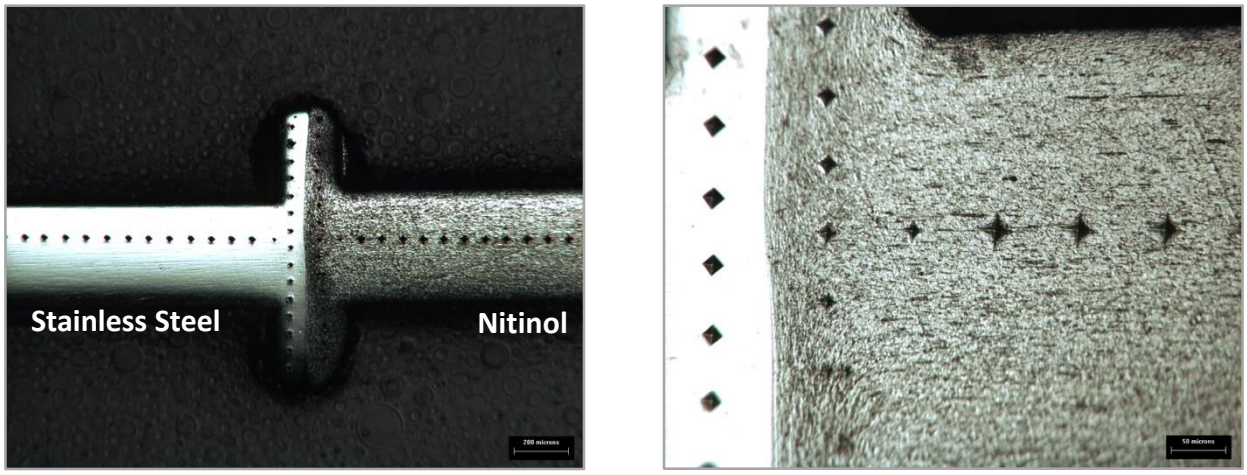

(a) (b)

Figure 24. Process B guide wire (a) 50x magnification (b) 200x magnification. In both micrographs, the Nitinol section is the darker portion of the wire, on the right side of each image.

Guide wires are for both process types were welded, then ground to specified diameters. This means that the length of the HAZ was likely similar within the two process groups. Grinding the diameters of the wires to smaller values, may be increasing the ratio of the length of the softer heat-affected zone to the ratio of the cross sectional area of the weld interface. The strength of the stainless steel portion of wire supports the weld, so decreasing the surface area interaction of the stainless steel and the Nitinol, while maintaining the length of the HAZ, may be contributing to the decrease in ultimate tensile strength that occurred with the decrease in grind diameter. Furthermore, there may be a difference in the length of the HAZ between the two process types, This may explain the lower ultimate tensile strengths produced by Process B. The effect of the ratio of HAZ length to wire diameter on microhardness of the guide wire welds, was not sufficiently tested in order to make conclusions as to how it affects the mechanical properties of the welds.

8. CONCLUSIONS

1. The process type affected the ultimate tensile strength of the 304 stainless steel - Nitinol joints in the guide wires. The mean ultimate tensile strength for Process A wires was 13.05 ksi higher than the mean ultimate tensile strength for Process B wires.

2. The grind diameter affected the ultimate tensile strengths mechanical properties of the 304 stainless steel - Nitinol joints in the guide wires. The mean ultimate tensile strength of 0.0125" wires was 9.25 ksi higher than mean ultimate tensile strength of the 0.0085" wires, and was 19.37 ksi higher than the mean ultimate tensile strength of the 0.0055" wires.

3. The values for microhardness did not appear to show a trend in the transverse direction, across the wire diameter near the weld. The microhardness values in the longitudinal direction were lower near the weld interface in the heat-affected zone, and then increased as measurements moved further away from the weld.

9. REFERENCES

[1] A. Epstein, "Impact of Minimally Invasive Surgery on Medical Spending and Employee Absenteeism," *JAMA Surgery*, Vols. 148, No. 7, no. 2013, pp. 641-647, 2013.

[2] D. Fornell, "The Basics of Guide Wire Technology," 2011. [Online]. [Accessed 29 October 2015].

[3] H. Hermawan and D. Ramdan, "Metals for Biomedical Applications," Malaysia.

[4] P. P. Poncet, "Nitinol Medical Device Design Considerations," Menlo Park, CA.

[5] A. R. Pelton and S. M. Russell, "The Physical Metallurgy of Nitinol for Medical Applications," *Journal of Metals*, pp. 33-37, 2003.

[6] R. A. Covert and A. H. Tuthill, "Stainless Steels: An Introduction to Their Metallurgy and Corrosion Resistance," *Dairy, Food and Environmental Sciences*, Vols. 20, No. 7, pp. 506, 517.

[7] T. Haas and A. Schuessler, "Welding and Joining of TiNi Shape Memory Alloys: Engineering Aspects and Medical Applications," in *First European Conference on Shape Memory and Superelastic Technologies*, Antwerp Zoo, 1999.

[8] Memry Corporation , "Fabrication of Nitinol Materials and Components," in *International Conference on Shape Memory and Superelastic Technologies*, China.

[9] S. Leonard, "Welding Technology Fuses Nitinol to Stainless Steel," *Medical Manufacturing News*, Vols. 31, No. 5, 2007.

[10] R. M. Miranda, "Dissimilar Laser welding of NiTi to Stainless Steel and Ti alloys," in *Workshop Processing, Characterization and Applications of Shape Memory Alloys*.

[11] "Flash Butt Welding in the UK," [Online]. [Accessed 1 December 2015].

[12] S. Tsang, "Friction Welding, Welding, Brazing, and Soldering," in *ASM Handbook*, vol. 6, ASM International, 1993, pp. 315-317.

[13] "Modern Grinding - Medical Wire Manufacturing," [Online]. [Accessed 30 October 2015].

[14] T. Santonen and H. Stockmann-Juvala, "Review on Toxicity of Stainless Steel," 2010.

10. APPENDICES

10.1 Appendix A: Tensile Testing Data

Table V. Tensile Testing Data

GROUP	PROCESS TYPE	SAMPLE NUMBER	DIAMETER (inch)	Date Tested	Max Load (lbf)	UTS (ksi)
Group 1	A	1	0.01246	3/4/16	22.76	186.68
Group 1	A	3	0.01244	4/26/16	23.44	192.82
Group 1	A	5	0.01243	3/5/16	24.10	198.62
Group 1	A	9	0.0124	3/5/16	23.68	196.09
Group 1	A	11	0.01248	4/26/16	23.24	189.97
Group 1	A	12	0.0124	3/5/16	23.17	191.85
Group 1	A	14	0.01241	4/12/16	22.53	186.27
Group 1	A	15	0.01244	3/5/16	23.57	193.96
Group 1	A	16	0.01248	4/26/16	23.90	195.36
Group 1	A	18	0.01243	4/29/16	22.99	189.46
Group 2	A	19	0.00848	5/1/16	10.47	185.43
Group 2	A	20	0.00854	4/28/16	10.08	175.91
Group 2	A	21	0.00847	5/1/16	10.54	187.08
Group 2	A	22	0.00848	4/29/16	10.20	180.51
Group 2	A	23	0.00848	4/30/16	10.36	183.47
Group 2	A	24	0.00851	3/5/16	10.31	181.21
Group 2	A	25	0.00848	3/4/16	10.48	185.47
Group 2	A	26	0.00849	3/4/16	9.94	175.60
Group 2	A	27	0.00851	4/26/16	10.40	182.81
Group 2	A	28	0.00854	4/20/16	10.46	182.56
Group 3	A	29	0.00551	5/1/16	4.39	183.90
Group 3	A	30	0.00555	4/12/16	4.09	169.06
Group 3	A	31	0.00555	4/20/16	4.28	176.71
Group 3	A	32	0.00554	5/1/16	4.14	171.87
Group 3	A	34	0.00554	4/29/16	4.05	167.85
Group 3	A	35	0.00553	4/12/16	4.13	171.91
Group 3	A	36	0.00553	4/26/16	4.31	179.36
Group 3	A	37	0.00552	4/30/16	4.16	173.91
Group 3	A	38	0.00555	4/30/16	4.30	177.54
Group 4	B	39	0.01433	4/28/16	28.84	178.82

Group 4	B	40	0.01434	3/5/16	30.42	188.36
Group 4	B	42	0.01431	4/28/16	28.70	178.42
Group 4	B	45	0.01435	5/1/16	29.38	181.64
Group 4	B	46	0.0143	4/30/16	30.39	189.19
Group 4	B	48	0.01432	3/4/16	29.41	182.58
Group 4	B	51	0.01434	3/5/16	29.36	181.79
Group 4	B	53	0.01429	3/5/16	30.51	190.23
Group 4	B	54	0.0143	4/30/16	28.88	179.84
Group 4	B	55	0.01432	4/20/16	28.78	178.72
Group 5	B	57	0.01224	4/29/16	20.72	176.11
Group 5	B	58	0.01225	4/28/16	21.32	180.88
Group 5	B	59	0.01232	4/29/16	20.71	173.72
Group 5	B	60	0.01226	4/28/16	21.51	182.23
Group 5	B	61	0.01226	4/20/16	21.92	185.71
Group 5	B	62	0.01226	4/20/16	20.85	176.64
Group 5	B	63	0.01224	3/5/16	21.76	184.94
Group 5	B	64	0.01225	4/20/16	21.12	179.23
Group 5	B	65	0.01228	4/30/16	21.29	179.74
Group 5	B	66	0.01224	4/29/16	21.03	178.71
Group 6	B	67	0.00829	4/30/16	9.01	166.85
Group 6	B	68	0.0083	4/28/16	9.12	168.47
Group 6	B	69	0.00831	4/30/16	9.49	175.05
Group 6	B	70	0.00829	4/30/15	9.29	172.02
Group 6	B	71	0.00831	4/12/16	9.30	171.45
Group 6	B	72	0.00831	5/1/16	9.18	169.17
Group 6	B	73	0.00834	4/20/16	9.21	168.61
Group 6	B	74	0.0083	4/28/16	9.48	175.19
Group 6	B	75	0.0083	4/30/16	9.30	171.92
Group 6	B	76	0.0083	3/4/16	9.48	175.16
Group 7	B	77	0.00548	4/12/16	3.76	159.59
Group 7	B	78	0.00544	4/26/16	3.75	161.25
Group 7	B	79	0.00539	4/26/16	3.50	153.57
Group 7	B	80	0.0054	4/30/16	3.60	157.32
Group 7	B	82	0.00541	4/12/16	3.72	161.92
Group 7	B	83	0.00548	4/20/16	3.87	163.95
Group 7	B	84	0.00535	4/30/16	3.53	157.12
Group 7	B	85	0.00546	4/26/16	3.62	154.61
Group 7	B	86	0.00542	5/1/16	3.62	156.94

10.2 Appendix B: Microhardness Data

Meas. Order 1 in Tables 6 and 7 refer to the order that microhardness indentations were made in the transverse directions. The indentations were made from one diameter side, to the other. Meas. Order 2 in Tables 6 and 7 refer to the order that microhardness measurements were made in the longitudinal direction. The first longitudinal measurements were closest to the weld. Subsequent measurements moved further away from the weld with each order number.

Table VI. Microhardness Data for Process A Wire

Meas. Order 1	Meas. Order 2	Region	Direction	Material	Load (gf)	Horizontal (D1) (microns)	Vertical (D2) (microns)	D_{ave} (microns)	HV
N/A	1	1	Longitudinal	NiTi	100	25.25	24.25	24.75	302.73
N/A	2	1	Longitudinal	NiTi	300	41.75	40	40.875	332.97
N/A	3	1	Longitudinal	NiTi	300	39.5	42	40.75	335.02
N/A	4	1	Longitudinal	NiTi	300	40	41.3	40.65	336.67
N/A	5	1	Longitudinal	NiTi	300	41	41.8	41.4	324.58
N/A	6	1	Longitudinal	NiTi	300	40.5	40.75	40.625	337.08
N/A	7	1	Longitudinal	NiTi	300	39.75	40.5	40.125	345.54
N/A	8	1	Longitudinal	NiTi	300	40.5	41.25	40.875	332.97
N/A	9	1	Longitudinal	NiTi	300	40.5	40.2	40.35	341.69
N/A	10	1	Longitudinal	NiTi	300	38.75	41	39.875	349.88
N/A	11	1	Longitudinal	NiTi	300	40.25	41	40.625	337.08
N/A	12	1	Longitudinal	NiTi	300	39.75	41.25	40.5	339.17
N/A	13	1	Longitudinal	NiTi	300	39.75	41.5	40.625	337.08
N/A	1	4	Longitudinal	SS	100	19.5	19.5	19.5	487.68
N/A	2	4	Longitudinal	SS	300	29	30	29.5	639.26
N/A	3	4	Longitudinal	SS	300	30.5	30	30.25	607.96
N/A	4	4	Longitudinal	SS	300	30.25	30.75	30.5	598.03
N/A	5	4	Longitudinal	SS	300	30.25	30.75	30.5	598.03
N/A	6	4	Longitudinal	SS	300	29	29.25	29.125	655.83
N/A	7	4	Longitudinal	SS	300	29.75	29.5	29.625	633.88
N/A	8	4	Longitudinal	SS	300	30	29.5	29.75	628.57
N/A	9	4	Longitudinal	SS	300	29.75	29.25	29.5	639.26
N/A	10	4	Longitudinal	SS	300	29.75	29.5	29.625	633.88

N/A	11	4	Longitudinal	SS	300	31.75	32.25	32	543.28
N/A	12	4	Longitudinal	SS	300	29.75	29.5	29.625	633.88
N/A	13	4	Longitudinal	SS	300	28.75	29.5	29.125	655.83
1	N/A	2	Transverse	NiTi	100	24.5	25.75	25.125	293.76
2	N/A	2	Transverse	NiTi	100	25.25	24.25	24.75	302.73
3	N/A	2	Transverse	NiTi	100	25.25	24	24.625	305.81
4	N/A	2	Transverse	NiTi	100	23.75	24.25	24	321.94
1.5	N/A	2	Transverse	NiTi	100	24.75	23.5	24.125	318.62
2.5	N/A	2	Transverse	NiTi	100	24.75	23.5	24.125	318.62
3.5	N/A	2	Transverse	NiTi	100	24.5	24	24.25	315.34
1	N/A	3	Transverse	SS	100	21	22	21.5	401.17
2	N/A	3	Transverse	SS	100	19.5	19.5	19.5	487.68
3	N/A	3	Transverse	SS	100	19.5	20.25	19.875	469.45
4	N/A	3	Transverse	SS	100	21.25	23	22.125	378.82
1.5	N/A	3	Transverse	SS	100	21.5	22.5	22	383.14
2.5	N/A	3	Transverse	SS	100	20.5	22.5	21.5	401.17
3.5	N/A	3	Transverse	SS	100	22.5	22.5	22.5	366.30

Table VII. Microhardness Data for Process B Wire

Meas. Order 1	Meas. Order 2	Region	Direction	Material	Load (gf)	Horizontal (D1) (microns)	Vertical (D2) (microns)	D_{ave} (microns)	HV
N/A	1	1	Longitudinal	NiTi	100	24.75	24.75	24.75	302.73
N/A	2	1	Longitudinal	NiTi	300	38.75	41	39.875	349.88
N/A	3	1	Longitudinal	NiTi	300	39.75	40.25	40	347.70
N/A	4	1	Longitudinal	NiTi	300	39	41	40	347.70
N/A	5	1	Longitudinal	NiTi	300	38.5	41.25	39.875	349.88
N/A	6	1	Longitudinal	NiTi	300	39.75	41.25	40.5	339.17
N/A	7	1	Longitudinal	NiTi	300	40.75	41	40.875	332.97
N/A	8	1	Longitudinal	NiTi	300	40.5	42	41.25	326.95
N/A	9	1	Longitudinal	NiTi	300	40	40	40	347.70
N/A	10	1	Longitudinal	NiTi	300	40	41	40.5	339.17
N/A	11	1	Longitudinal	NiTi	300	40	41.4	40.7	335.84
N/A	12	1	Longitudinal	NiTi	300	40.5	40.5	40.5	339.17
N/A	13	1	Longitudinal	NiTi	300	38.5	39.75	39.125	363.43
1	N/A	2	Transverse	NiTi	100	28.5	31.5	30	206.04

2	N/A	2	Transverse	NiTi	100	25.75	25.5	25.625	282.41
3	N/A	2	Transverse	NiTi	100	25.75	26.5	26.125	271.70
4	N/A	2	Transverse	NiTi	100	26.2	26.5	26.35	267.08
5	N/A	2	Transverse	NiTi	100	25.25	25.75	25.5	285.18
6	N/A	2	Transverse	NiTi	100	23.5	25	24.25	315.34
7	N/A	2	Transverse	NiTi	100	25.5	25.25	25.375	288.00
8	N/A	2	Transverse	NiTi	100	26	26	26	274.32
9	N/A	2	Transverse	NiTi	100	26.2	25.5	25.85	277.51
11	N/A	2	Transverse	NiTi	100	24.75	26	25.375	288.00
12	N/A	2	Transverse	NiTi	100	26	25.75	25.875	276.98
13	N/A	2	Transverse	NiTi	100	25.5	25.5	25.5	285.18
14	N/A	2	Transverse	NiTi	100	25.5	27	26.25	269.12
15	N/A	2	Transverse	NiTi	100	26.5	27	26.75	259.15